Molecular Immunology 107 (2019) 21–28

Contents lists available at ScienceDirect

Molecular Immunology

journal homepage: www.elsevier.com/locate/molimm

ZAP70 deficiency promotes reverse cholesterol transport through MAPK/ERK pathway in Jurkat cell

Jichen Liu, Kai Guo, Lu Hu, Tiantian Luo, Yusheng Ma, Yanan Zhang, Wenyan Lai, Zhigang Guo*

Department of Cardiology, Huiqiao Medical Center, Nanfang Hospital, Southern Medical University, Guangzhou 510515, Guangdong, People's Republic of China

ARTICLE INFO

Keywords:
Reverse cholesterol transport
ZAP70
T cells
ERK

ABSTRACT

Background: Lots of studies have demonstrated that immune cells could regulate reverse cholesterol transport (RCT). However, neither T cell receptor (TCR) signalling nor Zeta-chain associated protein 70 (ZAP70) have been demonstrated to be associated with RCT. To investigate this association, we used a ZAP70-deficient Jurkat-derived mutant, P116 cell line, to detect the effect of ZAP70 on RCT and inflammatory response. ZAP70 deficiency improved cholesterol efflux capacity by 14%. Meanwhile, mRNA and proteins expression of RCT regulatory proteins such as ABCA1, ABCG1 and SR-BI were increased in P116 cells. ZAP70-deficiency had no influence on LXR-α and PPAR-γ. Regarding the inflammatory response, the mRNA expression and secretion of pro-atherosclerotic cytokines, TNF-α, IFN-γ, IL-2 and IL-6, were significantly decreased in the ZAP70-deficient cell line. Activation of MAP kinases cascades, as determined by of ERK, JNK and p38 MAPK phosphorylation, were found to be inhibited in the absence of ZAP70. Specific inhibition of ERK, JNK and p38 MAPK activity was also found to decreased TNF-α, IFN-γ, and IL-6 secretion. However, only the ERK inhibition was observed to reduce IL-2 secretion, improve cholesterol efflux capacity and increase expression of ABCA1, ABCG1 and SR-BI without increasing LXR-α and PPAR-γ. Using ChIP assay to detect the binding of LXR-α to LXRE, which promotes the expression of ABCG1, we found that inhibiting ERK improved binding without increasing LXR-α levels. Thus, we speculate that ZAP70-deficiency may improve RCT and decrease the inflammatory response of T cells. Furthermore, these effects are probably achieved via ERK signalling pathway.

1. Introduction

Cardiovascular disease (CVD) is the major cause of death worldwide, and the principal contributing factor to the CVD pathology is atherosclerosis, which is characterized by the accumulation of low-density lipoprotein (LDL) and inflammatory cells, mainly macrophages and T cells (McLaren et al., 2011). Atherosclerosis is a well-known chronic, inflammatory disorder disease (Ross, 1999). Both innate and adaptive the immune responses modulate the development of atherosclerosis, such as lesion initiation and progression, and potentially devastating thrombotic complications. Inflammatory response disorders could also impair reverse cholesterol transport (RCT) which helps remove the cholesterol deposited in artery lesions. Aside from macrophages, T cells are known to play an important role in regulating the development of atherosclerosis (McLaren et al., 2011). Some studies have found that immuno-deficient mice, lack of T-cell and conventional B-cell populations, that carry a severe combined immunodeficiency mutation (SCID) when crossed with ApoE- or LDLR-deficient mice have a progeny with less advanced atherosclerosis progression (Daugherty et al., 1997). Transfer of $CD4^+$ T cells from ApoE-deficient mice to ApoE-deficient SCID mice resulted in significantly enhanced atherosclerosis progression (Zhou et al., 2000). Additionally, treatment with effector T cells (Teff) derived from systemic lupus erythematous (SLE)–susceptible mice stimulated atherosclerosis in of Rag/LDLR-deficient mice (Wilhelm et al., 2015).

The T cell receptor (TCR) pathway is associated with T cell activation and differentiation. When specific antigen peptides are recognized by the TCR, lymphocyte-specific protein tyrosine kinase (lck) phosphorylates the immune-receptor tyrosine-based activation motifs (ITAMs) of the TCR-CD3 complex and at the meantime recruits Zeta-chain associated protein 70 (ZAP70) to the doubly phosphorylates ITAMs. ZAP70 then phosphorylates its downstream substrates, promotes activation and differentiation of T cells and secretion of inflammatory factors (Hashimoto-Tane and Saito, 2016).

ZAP70 is a spleen tyrosine kinase (Syk) family tyrosine kinase expressed predominantly in T and natural killer cells. ZAP70 is composed of a carboxyl-terminal kinase domain and two SH2 domains which bind to doubly phosphorylated ITAMs of TCR zeta-chain. In resting T cells,

* Corresponding author.
E-mail address: guozhigang126@126.com (Z. Guo).

https://doi.org/10.1016/j.molimm.2019.01.001
Received 1 March 2018; Received in revised form 12 December 2018; Accepted 2 January 2019
Available online 10 January 2019
0161-5890/

ZAP70 is distributed throughout the cytoplasm, but is rapidly recruited to the plasma membrane following TCR stimulation and ITAM phosphorylation. ZAP70 then activates downstream pathways like Mitogen-activated protein kinases (MAPK) signalling pathway, Ca^{2+}-NEAF- IL-2 pathway and nuclear factor-κB (NF-κB) (Wang et al., 2010). ZAP70 plays a critical role in cell surface expression of T cell antigen receptor-CD3 complex signalling during the early stages of T cell development and differentiation, activation and immune response. The development of thymocyte in ZAP70-deficient mice is arrested at the double positive (DP) stage and secondary peripheral lymphoid tissues are found completely absence of both $CD4^+$ and $CD8^+$ T cells (Negishi et al., 1995). Moreover, lack of functional ZAP70 results in a marked reduction in protein tyrosine phosphorylation, calcium flux, activation of T cell and secretion of inflammatory factors (Au-Yeung et al., 2009).

Our previous study has indicated that the TCR signalling pathway was associated with reduced cholesterol efflux capacity, which was mediated by HSP65-induced T cells. Silencing both lck and ZAP70 rescued the cholesterol efflux capacity and increased the expression of RCT regulatory proteins which down-regulated by HSP65 (Hu et al., 2018; Luo et al., 2016). We also found that silencing ZAP70 could regulate HSP65-induced T cell proliferation and NF-kB activation. However, the signalling pathway that acts downstream of ZAP70 in RCT remains unknown. Our study aimed to investigate the effect of ZAP70 on RCT and inflammation and how ZAP70 influences RCT. These results may help to clarify the connection between inflammation and cholesterol metabolism.

2. Material and methods

2.1. Reagents and antibodies

[^{3}H] cholesterol was purchased from PerkinElmer (Shanghai, China). ApoA–I was acquired from Calbiochem (Darmstadt, Germany). Functional-grade, purified anti-CD3 and anti-CD28 (clones HIT3a and CD28.2, respectively) antibodies were obtained from eBioscience. Inflammatory factors, TNF-α, IFN-γ IL-2 and IL-6, were tested by ELISA kits (Cusabio Biotech). Antibodies against ABCA1 (ab66217), ABCG1 (ab52617), SR-BI (ab106572), PPAR-γ(ab191407), LXR-α (ab176323) were acquired from Abcam. Antibodies against phosphorylated (Thr202/Tyr204, 9101) and non-phosphorylated ERK (4695) phosphorylated (Thr183/Tyr185, 4668) and non-phosphorylated JNK (9252), phosphorylated (Thr180/Tyr182, 4511) and non-phosphorylated p38 (8690) and ZAP70 (2705) were acquired from Cell Signalling Technology. Western blot stripping buffer was acquired from Thermo Scientific (46,430). A PrimeScript reverse transcription reagent kit and quantitative PCR mix were acquired from TaKaRa. Inhibitors of ERK (U0126), JNK (SP600125) and p38 (SB203580) were purchased from Selleck. ChIP assay was acquired from Pierce.

2.2. Cell lines, culture conditions, and cell stimulation

Jurkat cells (human acute T lymphocyte leukemia cell lines and CCTCC) and the ZAP70-deficient Jurkat-derived mutant, P116 (ATCC) were cultured in complete RPMI (RPMI 1640 supplemented with 10% heat- inactivated fetal calf serum (FCS), 2 mM L-glutamine, 50U penicillin/ml, 50 μg streptomycin/ml (all from Life Technologies) at 37° C in 5% CO2. All the groups of Jurkat cells and P116 were stimulated with anti-CD3 and anti-CD28 (0.5 ug/1*10^6 cells) for 24 h. Different inhibitor groups were treated U0126(10 μM) or SP600125(10 μM) or SB203580 (10 μM) for 0.5 h before treatment with anti-CD3 and anti-CD28.

2.3. Western blot analysis and quantification

Proteins of Jurkat and P116 cells were extracted with radio-immunoprecipitation assay (RIPA) lysis buffer containing protease inhibitors or phosphatase inhibitors. Proteins resolved on polyacrylamide gels were transferred onto PVDF membranes (Millipore) and blocked for 1 h in 5% non-fat milk at room temperature. Blots were then incubated over night with specific primary antibodies at 4 °C and washed, followed by a 1-h incubation with secondary antibodies conjugated to HRP at room temperature. Target proteins were recorded by using enhanced chemiluminescence (ECL) reagents and quantified using the ImageJ software. Subsequently, blots probed phosphor-antibodies were stripped by stripping buffer (ThermoFisher). Blots were re-incubated with secondary HRP-conjugated antibodies and exposed to film to confirm that the phospho-antibodies had been successfully removed. Then the blots were re-probe for the corresponding total protein antibodies. The protein of β-Actin protein expression was used as the internal reference.

2.4. Assessment of cholesterol efflux capacity

Jurkat and P116 cells were stimulated or blocked as above mentioned, then were plated and incubated in RPMI 1640 medium with 0.5% BSA, 30 mg/ml ox-LDL and 1 μCi/ml [1α,2α-^{3}H]-cholesterol for 24 h. After washing with serum-free RPMI 1640 medium, the cells were then incubated in 1640 with 0.5%BSA with or without 10 mg/ml apolipoprotein A-I (apo A-I) for 6 h. The incubation medium was collected and the cells were washed with PBS and then lysed with 0.1 M NaOH. Finally, the radioactivity of the medium and the cell lysate was measured using liquid scintillation spectrometry. The percent efflux was calculated by the following formula:

[micro-curies of ^{3}H-cholesterol in mediums ÷ (micro-curies of ^{3}H-cholesterol in cells + micro-curies of ^{3}H-cholesterol in mediums)] ×100.

2.5. Quantitative real-time PCR

Total mRNA was extracted using TRIzol reagent (Invitrogen, Gaithersburg, MD) in accordance with the manufacturer's instructions and reverse transcribed using a PrimeScript™RT Reagent Kit (TaKaRa, China). Real-time quantitative PCR (qPCR) was performed on a LightCycler 480 II (Roche, Switzerland) with a SYBR Premix Ex Taq kit (TaKaRa, China). The level of β-actin mRNA expression was used as the internal reference. Data are presented as the fold change over the control group, as determined using the $^{\triangle\triangle}$Ct method.

2.6. Chromatin immunoprecipitation (ChIP) assay

ChIP assays were measured as described previously (Sabol et al., 2005). Briefly, after treatment, the cells were cross-linked with 1% formaldehyde for 10 min at room temperature. Nuclei were isolated and sonicated on ice to shear the chromatin into fragments of 200–1200 bp (average 500 bp). The input PCR was conducted with DNA extracted from the sonicated chromatin after reversal of the cross-linking. Immunoprecipitation was conducted with the same amount of chromatin from each sample based on the input and rabbit anti-LXR polyclonal antibody, followed by PCR. The primers for the ChIP assay were as follows: LXRE-A, GAAGTCAGCAGGGCTCAGC, AGGATGCAGTTGTCAC AGCG; LXRE-B, TCTTGCCCGAGCTCAACG, GTTACTAGCGAGCGTTGA CCG

2.7. Statistical analysis

Data are expressed as the mean ± SD. Statistical analyses were performed using SPSS statistics. All data were collected from at least three biological replicates, with two experimental replicates per group. Statistical analysis was conducted using a 2-tailed Student's *t*-test or one-way ANOVA followed by the Bonferroni–Dunn post hoc test. A P value

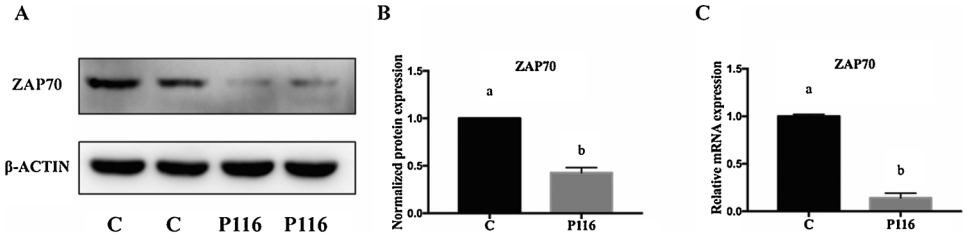

Fig. 1. ZAP70 expression comparison in Jurkat and P116 cells.
Jurkat and P116 cells were incubated with anti-CD3 and anti-CD28 antibodies (0.5 μg/ml) for 24 hours. A and B, Expression of ZAP70 was assessed by Western blot and quantified with Image. Representative images from 3 biological replicates with 2 experimental replicates, are shown. All data were quantified, and the results are shown in B. C, Expression of ZAP70 mRNA expression. *P < 0.05 compared with Jurkat cell group; N (biological versus experimental replicates) = 6 vs 2. All data areexpressed as the mean ± SD. C, Jurkat cells; P116, P116 cells. Data that were not significantly different (P > 0.05) are indicated with the same letter (two-tailed unpaired t-test).

(two-tailed) of 0.05 or less was considered to be statistically significant.

3. Results

3.1. ZAP70 deficiency improve cholesterol efflux capacity and increase expression of RCT regulatory proteins

A previous study from our research team showed that cholesterol efflux capacity was increased and the expression of cholesterol transportation regulatory proteins were upregulated in Jurkat cells after silencing lck and ZAP70, which are critical for TCR signal activation. To reconfirm the effect of ZAP70 on RCT, we used the P116 cell line which is a ZAP70-deficient Jurkat-derived mutant cell line (Fig. 1). We radiolabelled cholesterol in cell with ^{3}H-cholesterol and harvested activated Jurkat and P116 cells to assess the expression of cholesterol transportation regulatory proteins. Consistent with the previous report (Hu et al., 2018), we also found that absence of ZAP70 improved the cholesterol efflux capacity (control vs P116, 10.14% vs 24.89%, P < 0.001) (Fig. 2A) and upregulated the mRNA (Fig. 2B) and proteins level of the cytomembrane proteins, including ATP-binding cassette transporter A1 (ABCA1), ATP-binding cassette transporter G1 (ABCG1) and scavenger receptor B type I (SR-BI) (Fig. 2C and D). However, ZAP70 did not affect expression of liver X receptor α (LXR-α) or peroxisome proliferator-activated receptor γ (PPAR-γ), which are expressed in cell nucleus.

3.2. ZAP70 deficiency decreases inflammatory factor secretion through MAPK signalling inhibition

ZAP70 is essential for T cell proliferation and activation. We compared the ZAP70-mutant cells with jurkat cells to detect the effect of ZAP70-deficiency on T cell mediated inflammation, pro-inflammatory cytokines, tumor necrosis factor-α (TNF-α) (control vs P116, 246.5 vs 70.3 (pg/ml), P < 0.001), interferon-γ (IFN-γ) (control vs P116, 82.2

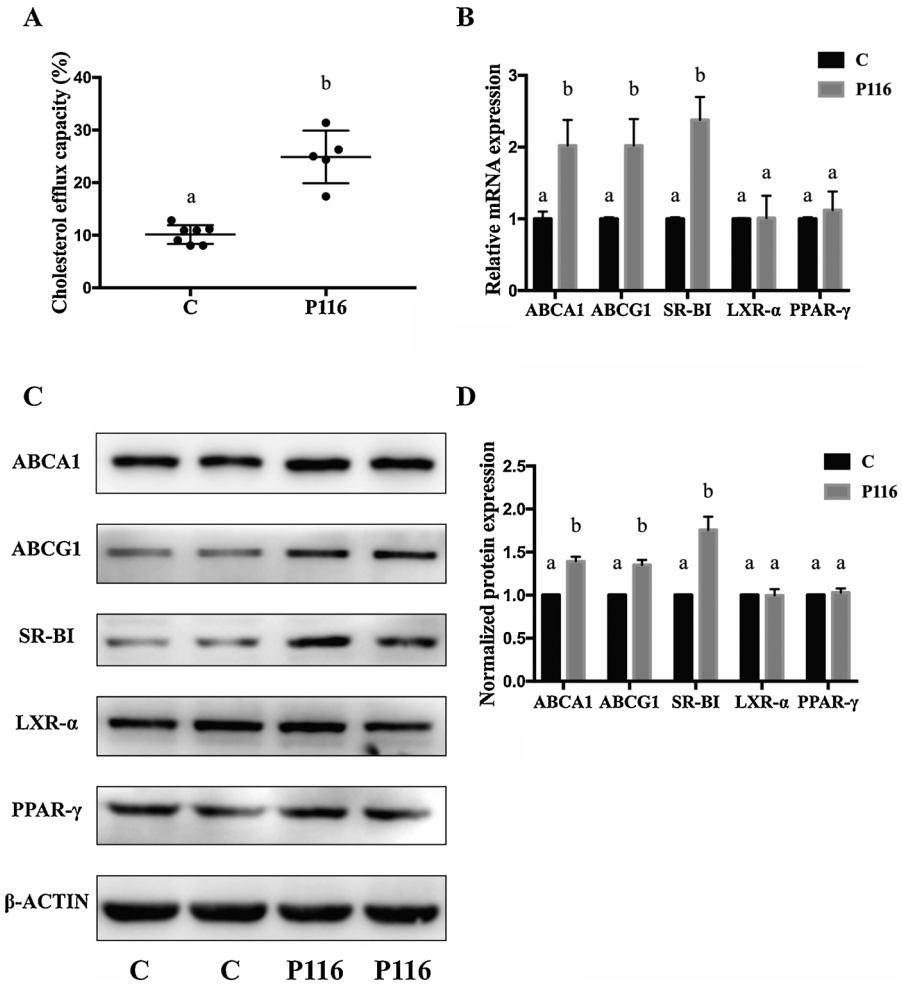

Fig. 2. Cholesterol efflux capacity and RCT regulatory proteins expression between Jurkat and P116 cells.
A, Cholesterol efflux capacity was detected with ^{3}H-cholesterol radioactivity using liquid scintillation spectrometry after Jurkat and P116 cells were stimulated with anti-CD3/CD28 antibodies and incubated with ox-LDL and ^{3}H-cholesterol for 24 hours, followed by incubation with apoA-I for 6 hours. N (biological versus experimental replicates) = 6 vs 2. B, RT-PCR analyzed mRNA of ABCA1, ABCG1, SR-BI, LXR-α and PPAR-γ, that were related to reverse cholesterol transport. N (biological versus experimental replicates) = 6 vs 2. C and D, Western blotting and quantification of cholesterol efflux regulatory protein expression.Representative images from 3 biological replicates and 2 experimental replicates are shown. All data were quantified, and the results are shown in D. Data that are not significantly different (P > 0.05) are indicated with the same letter (two-tailed unpaired t-test).

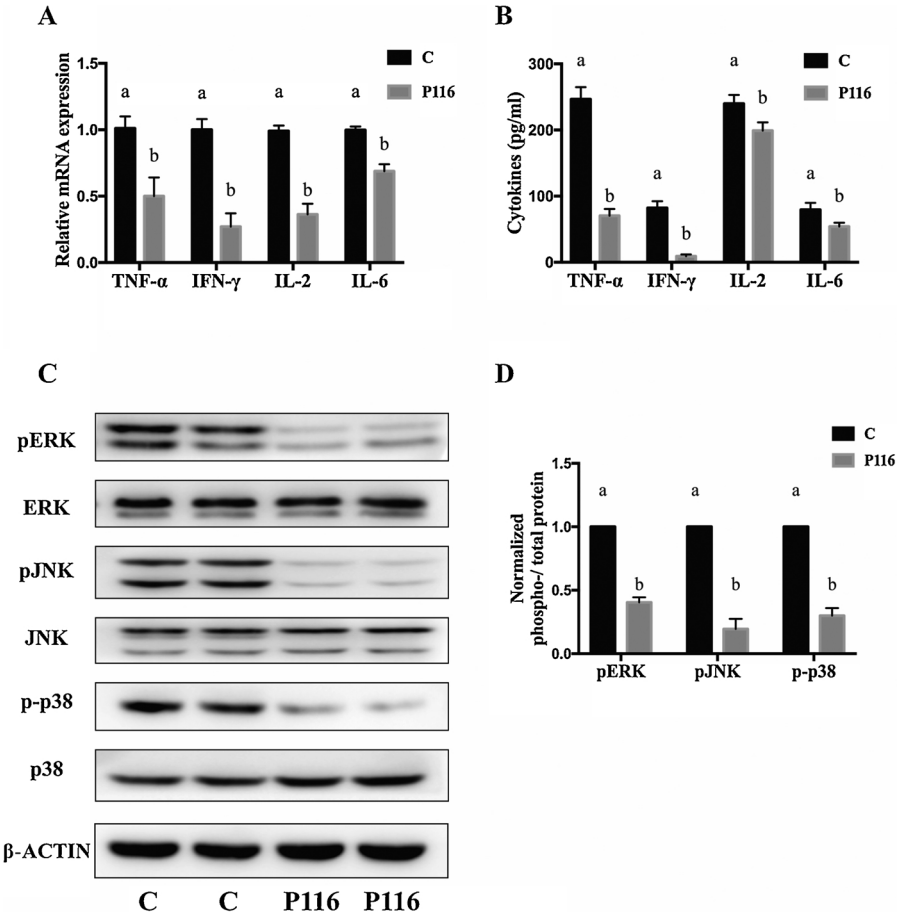

Fig. 3. Cytokines and inflammation related proteins expression between Jurkat and P116 cells.
A and B, ELISA was used to analyze cytokines (TNF-α, IFN-γ, IL-2 and IL-6) expression and RT-PCR was used to analyze mRNA of TNF-α and IFN-γ after Jurkat and P116 cells were stimulated with anti-CD3/CD28 antibodies for 24 hours. N (biological versus experimental replicates) = 6 vs 2. C and D, Protein and phosphorprotein levels of ERK, JNK and p38, which influenced inflammatory factors expression, were assessed by Western blot and quantified. Representative images from 3 biological replicates, with 2 experimental replicates, are shown. All data were quantified, and the results are shown in D. Data that are not significantly different ($P > 0.05$) are indicated with the same letter (two-tailed unpaired t-test).

vs 9.06 (pg/ml), $P < 0.001$), interleukin-2 (IL-2) (control vs P116, 239.9 vs 199 (pg/ml), $P < 0.05$) and IL-6 (control vs P116,79.43 vs 54.13 (pg/ml), $P < 0.05$). The results revealed that mRNA expression of TNF-α, IFN-γ, IL-2 and IL-6 were all down-regulated and their secretion were decreased owing to lacking ZAP70 (Fig. 3A and B). MAPK signalling pathway contain extracellular regulated protein kinases (ERK), c-Jun N-terminal kinases (JNK) and p38 MAPK which are phosphorylated and increased inflammatory response after T cell activated. We found that ZAP70 deficiency decreased ERK, JNK and p38 MAPK phosphorylation (Fig. 3C and D), probably indicating inflammatory response reduction. To determine the effect of ERK, JNK and p38 MAPK on inflammatory response, we used the specific inhibitors U0126, SP600125 and SB203580 to inhibit ERK, JNK and p38 MAPK phosphorylation, respectively, in Jurkat cells (Fig. 4A and B). We found that inhibiting ERK, JNK, p38 MAPK could all reduce the mRNA expression and secretion of TNF-α (control vs U0126 vs SP600125 vs SB203580, 246.5^a vs 83.6^b vs 79.8^b vs 120.5^c (pg/ml), Data that are not significantly different ($P > 0.05$) are indicated with the same letter, N (biological versus experimental replicates) = 3 vs 2), IFN-γ (82.2^a vs 23.9^b vs 38.1^c vs 41.5^c (pg/ml), Data that are not significantly different ($P > 0.05$) are indicated with the same letter) and IL-6 (79.43^a vs 56.54^b vs 51.69^b vs 47.81^b (pg/ml), Data that are not significantly different ($P > 0.05$) are indicated with the same letter). However, only inhibiting ERK could reduce the mRNA expression and secretion of IL-2 (239.86^a vs 181.07^b vs 236.73^a vs 226.77^a (pg/ml), Data that are not significantly different ($P > 0.05$) are indicated with the same letter) (Fig. 4C and D). Above all, the effects of ZAP70-deficiency on inflammatory factors are probably due to the inhibition of ERK, JNK and p38 MAPK phosphorylation.

3.3. Inhibiting ERK improved cholesterol efflux capacity and increased expression of RCT regulatory proteins

ZAP70 deficiency improves cholesterol efflux capacity and reduces MAP kinases phosphorylation. However, how ZAP70 affects cholesterol efflux capacity still remains unknown. To investigate whether the effect of ZAP70 on the cholesterol efflux capacity resulted from decrease of MAP kinases phosphorylation, we used different inhibitors respectively to block MAP kinases phosphorylation and evaluated the cholesterol efflux capacity and expression of RCT regulatory proteins and genes. The results revealed that inhibiting ERK phosphorylation could improve the cholesterol efflux capacity (control vs U0126, 10.1% vs 22.4%, $P < 0.05$, $N = 6$) (Fig. 5A). Likewise, inhibiting ERK phosphorylation could increase mRNA (Fig. 5B–D) and proteins (Fig. 6) expression of ABCA1, ABCG1 and SR-BI ($P < 0.05$). However, inhibitor of ERK had no effect on LXR-α and PPAR- γ. Neither JNK nor p38 MAPK had any effect on ABCA1, ABCG1, SR-BI, LXR-α and PPAR-γ mRNA (Fig. 5B–F) and protein (Fig. 6) expression ($P > 0.05$), indicating that JNK and p38 were not involved in RCT regulation (Fig. 7).

3.4. Inhibiting ERK improved the binding of LXR-α to LXRE to promote ABCG1 expression

Inhibiting ERK increased the expression of both protein and mRNA of ABCA1 and ABCG1. However, inhibiting ERK had no influence on LXR-α which was demonstrated to bind with LXR responsive elements (LXREs) in promoter of target gene, thereby activating its transcription. Sabol et al. identified two LXREs (LXRE-A and LXRE-B) in the first and second introns respectively of the human gene of ABCG1 which were demonstrated to be effective to bind with LXR-α and promote ABCG1 expression (Sabol et al., 2005). We therefore compared both LXRE-A

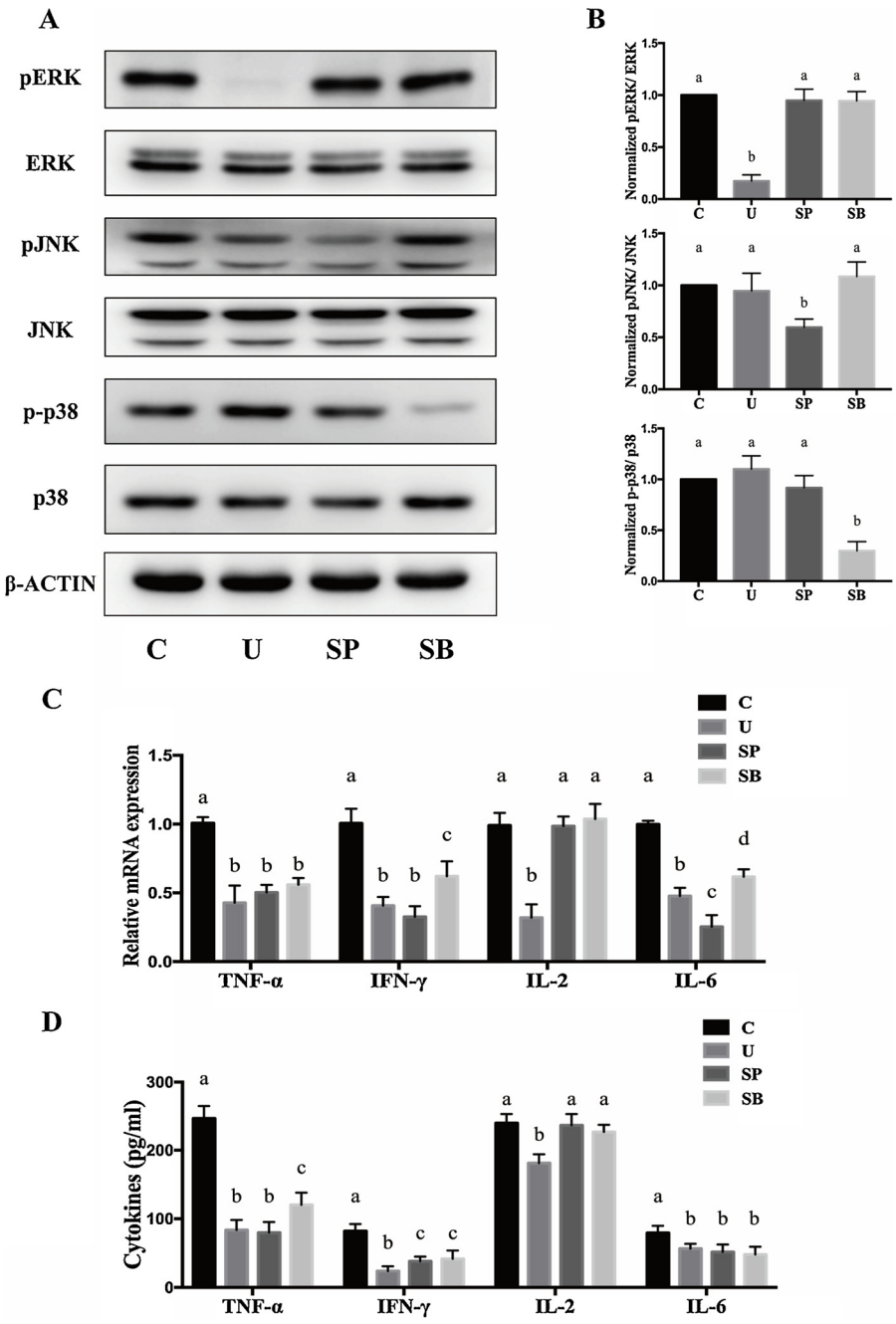

Fig. 4. Cytokines and inflammation-related proteins expression after Jurkat cells treated with different inhibitors.

Jurkat cells were treated with different inhibitors for 30 minutes and then stimulated with anti-CD3/CD38 antibodies for 24 hours. A and B, Protein and phosphor-proteins of ERK, JNK and p38 were assessed by Western blot and quantified. Representative images from 3 biological replicates, with 2 experimental replicates, are shown. All data were quantified, and the results are shown in B. C and D, Expression of cytokines (TNF-α, IFN-γ, IL-2 and IL-6) and their mRNA were analyzed by ELISA and RT-PCR. N (biological versus experimental replicates) = 6 vs 2. C represents the control group (Jurkat cell treated with DMSO,) U represents U0126 group (Jurkat cell treated with U0126 which inhibits phosphorylation of ERK), SP represents SP600125 group (inhibited phosphorylation of JNK) and SB represents SB203580 group (inhibited phosphorylation of p38). Data that are not significantly different ($P > 0.05$) are indicated with the same letter (one-way ANOVA).

and LXRE-B binding by LXR-α after treatment of ERK inhibitor with them in control group. ERK inhibition increased the interaction between LXR-α protein and LXRE-A. We didn't detect the binding of LXR-α to LXRE-B in Jurkat cells. Thus, inhibiting ERK appeared to increase ABCG1 expression by enhancing the binding of LXR-α to LXRE-A rather than by increasing LXR-α expression.

4. Discussion

Atherosclerosis is the principal cause of heart disease, myocardial infarction and stroke in Western society. Atherosclerosis is a chronic inflammatory disease triggered by the accumulation and retention of ApoB-containing lipoproteins, such as LDL and lipoprotein remnants, in the sub-endothelial intima. These trapped LDL were converted into modified forms, such as oxidized LDL (ox-LDL) which contribute to the inflammatory response and plaque development (Yu et al., 2013). Activation of lesion sites is followed by recruitment of predominantly circulating monocytes and T-cells, dysfunction of endothelial cell, formulation and accumulation of foam cells, and migration and proliferation of vascular smooth muscle cells. The accumulation of cholesterol and inflammatory response are essential to initiation and development of atherosclerosis (McLaren et al., 2011). RCT may help to remove accumulated cholesterol from cells in the sub-intima of the vessel wall through transporters (ABCA1, ABCG1, etc.) or other mechanisms such as passive diffusion, and then the cholesterol was collected by high-density lipoprotein (HDL) or apo A-I, and then transport cholesterol to hepatic cells for secretion of bile. The first step of RCT is cholesterol efflux from cells which is the most important for the anti-atherosclerotic extent (Hutchins and Heinecke, 2015). Cholesterol efflux capacity from cells, a new biomarker that characterizes a key step in reverse cholesterol transport, has a strong negative correlation with both carotid intima–media thickness and incidence of cardiovascular

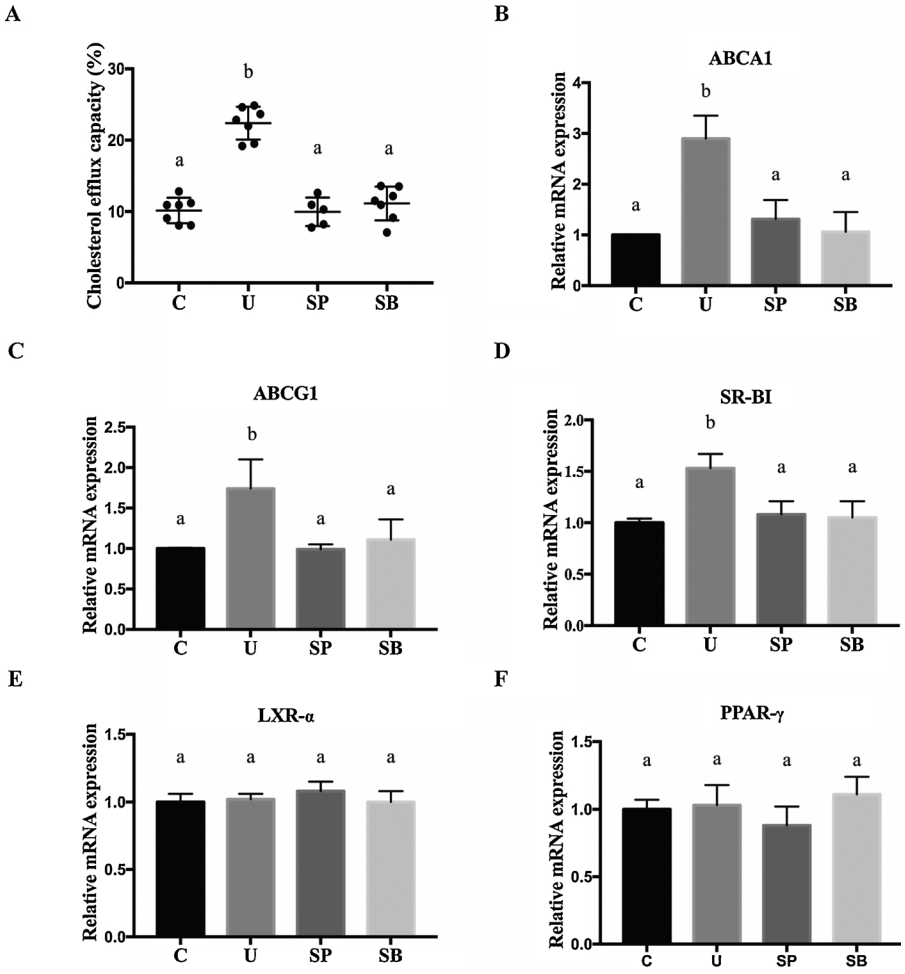

Fig. 5. Cholesterol efflux capacity and related gene expression after Jurkat cells treated with different inhibitors.

A, Jurkat cells were treated with different inhibitors for 30 minutes and incubated with anti-CD3/CD38 antibodies, ox-LDL and ^{3}H-cholesterol for 24 hours, followed by an incubation with apoA-I for 6 hours. ^{3}H-cholesterol radioactivity was detected by liquid scintillation spectrometry. B-F, Genes related to cholesterol efflux (ABCA1, ABCG1, SR-BI, LXR-α and PPAR-γ) were detected by RT-PCR. Data that are not significantly different ($P > 0.05$) are indicated with the same letter (one-way ANOVA), N (biological versus experimental replicates) = 6 vs 2.

events in a population-based cohort (Khera et al., 2011; Rohatgi et al., 2014). A lot of strategies enhancing cholesterol efflux capacity were demonstrated to be benefit of reducing atherosclerosis. RCT-enhancing therapies are currently considered a promising strategy for the prevention and treatment of atherosclerotic CVD (Bhatt and Rohatgi, 2016).

The development and activation of T cells play an important role in the progression of atherosclerosis. As for activation and differentiation of T cells, TCR signalling pathway is pivotal. ZAP70 plays a crucial role in formulation of TCR–microclusters, initiation of TCR signalling pathway, moreover activation of T cells and secretion of cytokines (Hashimoto-Tane and Saito, 2016). Thus, inhibition of ZAP70 by interacting with the TCR–CD3 may be effective for treating patients with autoimmune diseases, organ transplants or chronic inflammatory diseases. A previous study from our group found that lck, which regulates ZAP70 phosphorylation in TCR signalling, is associated with HSP65 inducing atherosclerosis. Down-regulating lck could enhance cholesterol efflux capacity of T cells (Luo et al., 2016). However, studies investigating the connection between ZAP70 and RCT or atherosclerosis are scarce. Previous study from our group showed that ZAP70 also regulated HSP65-induced RCT dysfunction (Hu et al., 2018). Using a ZAP70 mutant cell line, P116 cell line, we also demonstrated that ZAP70-deficiency had influence on RCT after activation of T cell by CD3/CD28. ZAP70 deletion significantly benefited RCT of T cells. Cholesterol efflux capacity, representative of RCT, was found remarkably improved in ZAP70-defient cells (Fig. 3A). Additionally, mRNA and proteins expression of ABCA1, ABCG1, SR-BI, which regulate RCT, were found increased in the ZAP70-mutant cell line (Fig. 3B–D). Together, these data demonstrated that ZAP70-deficiency could enhance RCT of T cells.

In addition to immune cells, cytokines could also regulate the development of atherosclerosis. Several novel strategies for inhibiting pro-atherosclerotic cytokines have been found to be effective for anti-atherosclerosis (Back and Hansson, 2015). Canakinumab, a monoclonal antibody binding to IL-1b and blocking IL-1b interaction with its receptor, was demonstrated be effective on reducing atherosclerosis. Recently, the CANTOS trial has reported that canakinumab at a dose of 150 mg every 3 months led to a significantly lower rate of recurrent cardiovascular events than placebo, independent of lipid-level lowering (Ridker et al., 2017). In our results, both mRNA and proteins secretion of pro-atherosclerotic cytokines, TNF-α, IFN-γ, IL-2 and IL-6, were found reduced in P116 cells compared with Jurkat cells (Fig. 2A and B). ZAP70 deficiency also reduced phosphorylation of ERK, JNK and p38 MAPK (Fig. 2C and D), which contributed to secretion of cytokines and activation of T cells. Besides, either lack of ZAP70 or inhibiting the phosphorylation of ERK, JNK and p38 MAPK with their specific inhibitors could reduce TNF-α, IFN-γ and IL6. Inhibiting the phosphorylation of ERK had additional effect of reducing IL-2 like lack of ZAP70. These findings demonstrated that ZAP70 deficiency reduces inflammatory regulatory pathway and secretion of inflammatory factors probably through MAPK pathway.

MAPK cascades are part of the downstream pathways of ZAP70 and have been shown to stimulate inflammatory response and promote progression of atherosclerosis (Muslin, 2008). Mouse peritoneal macrophages treated with ox-LDL were found that ERK1/2, p38 MAPK and JNK1/2 were all activated within 15 min, with ERK1/2 activation occurring at the earliest time point. Treating macrophages with JNK pathway inhibitor SP600125 blocked ox-LDL-induced foam cell

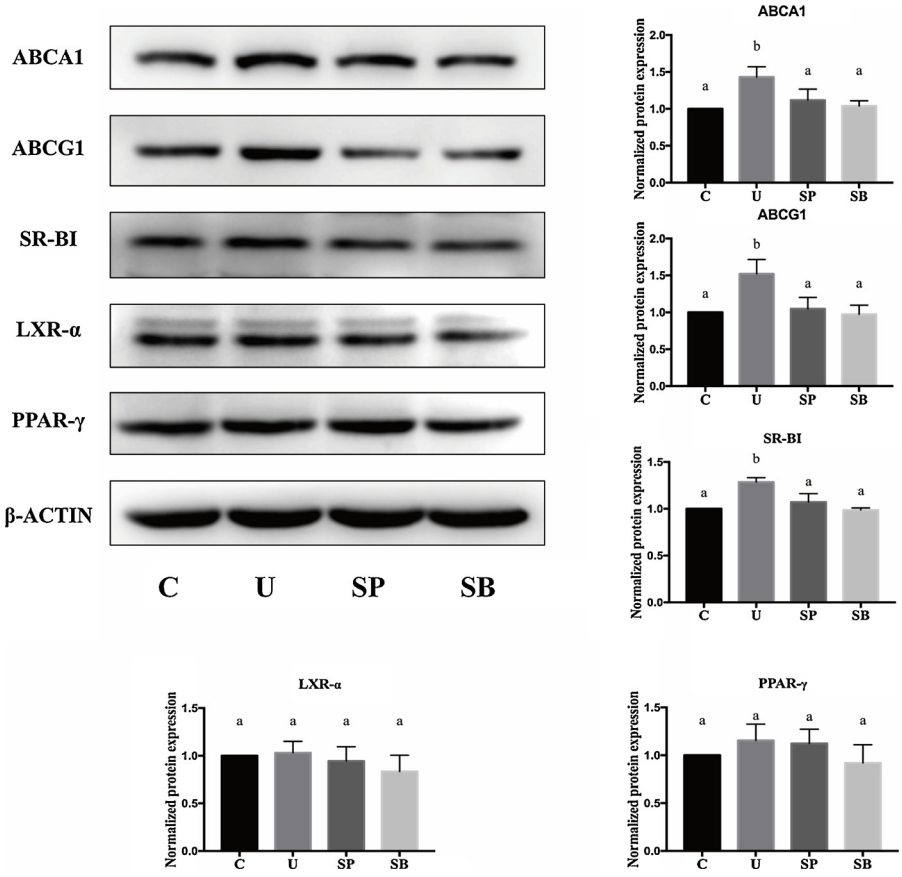

Fig. 6. Cholesterol efflux related proteins expression after cells were treated with different inhibitors.
Jurkat cells were treated with different inhibitors for 30 minutes and then stimulated with anti-CD3/CD38 antibodies for 24 hours. Proteins related to cholesterol efflux (ABCA1, ABCG1, SR-BI, LXR-α and PPAR-γ) were assessed by Western blot and quantified. Data that are not significantly different ($P > 0.05$) are indicated with the same letter (one-way ANOVA), Representative images from 3 biological replicates, with 2 experimental replicates, are shown. All data were quantified, and the results are shown in the figure.

formation (Rahaman et al., 2006). Another study found p38 MAPK inhibitor SB203580 had a similarly effect on foam cell formation in J774 macrophage cell line. Moreover, ApoE-/-mice treated with the p38 inhibitor SB203580 had reduced atheromatous lesions and decreased atherosclerotic disease progression (Seeger et al., 2010). Treating rat peritoneal macrophages with ERK inhibitor U0126 resulted in a marked reduction of lipid deposition, upregulation of ABCA1/G1 expression and suppression of CD36 expression in Ox-LDL-stimulated macrophages (Xue et al., 2016). Our study suggested that, ERK instead of JNK or p38 MAPK contributed to the increase of T-cell RCT. Treatment of U0126 enhanced cholesterol efflux capacity of T cells (Fig. 5A). Additionally, protein and mRNA expression of RCT regulatory proteins, ABCA1, ABCG1 and SR-BI, were increased after inhibiting ERK phosphorylation (Figs. 5 and 6). However, inhibiting JNK or p38 MAPK did not impact on cholesterol efflux capacity or the expression of RCT regulatory proteins. Together, these data demonstrated that ZAP70 make influence on RCT of T cells probably through ERK pathway.

ATP-binding cassette transporters such as ABCA1 and ABCG1 are expressed on cell membranes to transport cholesterol from cells to HDL. These transporters help to improve RCT and reduce atherosclerosis. ABCA1 and ABCG1 gene expression are primarily induced by the stimulation of liver X receptor/retinoid X receptor (LXR/RXR) axis, which is stimulated by cholesterol accumulation in the cells (Favari et al., 2015). LXR binds to the LXREs in the promoter of ABCG1 gene thereby activating its transcription (Zhang et al., 2016). Our study revealed that inhibiting ERK up-regulated ABCA1 and ABCG1 without increasing the expression of LXR-α. To examine this phenomenon in more detail, we used ChIP to detect LXRE binding with LXR-α. We found inhibiting ERK increased the interaction between LXR protein and the LXRE without increasing the amount of LXR-α. Together, we therefore concluded that inhibiting ERK increased ABCG1 expression by improving the binding of LXR-α to LXREs rather than through increased LXR-α expression.

In vivo, T cell functional phenotypes alter their relative ability to function as regulatory or inflammatory in response to environmental clues. Different T cell functional phenotypes could play different roles in atherosclerosis. An increase in the ratio of Teff to regulator T Cells (Treg) promotes atherosclerosis (Tabas and Lichtman, 2017). We found ZAP70-deficiency improves cholesterol efflux capacity and reduces inflammatory response of T cells. ZAP70-deficiency probably have influence on atherosclerosis owing to these effect. However, the effects of ZAP70-deficiency on neither ratio of Teff to Treg nor atherosclerosis in

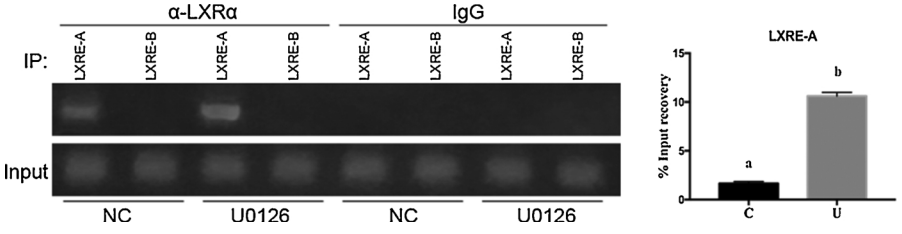

Fig. 7. ERK inhibition improved the binding of LXR-α to LXRE which promote ABCG1 expression.
Jurkat cells were treated with different inhibitors for 30 minutes and then stimulated with anti-CD3/CD38 antibodies for 24 hours. Cells were then used to isolate chromatin by sonication followed by immunoprecipitation with normal IgG or anti-LXR antibody as indicated. An isotype-matched IgG was used as a negative control. The PCR was conducted with the primers for the LXRE-A and LXRE-B which promote ABCG1 expression. Data that are not significantly different ($P > 0.05$) are indicated with the same letter (one-way ANOVA). Representative images from 3 biological replicates, with 2 experimental replicates, are shown. All data were quantified, and the results are shown in the figure.

vivo were not investigated in this paper. In the future, our group may continue to detect the effects of ZAP70-deficiency in vivo.

In conclusion, ZAP70-deficiency improves cholesterol efflux capacity, up-regulates RCT regulatory proteins and reduces inflammatory response in T cells. In addition, the ERK pathway probably contributes to these effects of ZAP70 by improving the binding of LXR-α to LXRE, thereby promoting ABCG1 expression.

Acknowledgements

This work was supported by the Science and Technology Foundation of Guangzhou City of China (2015010090), the Major Scientific Research Foundation of Colleges and Universities of Guangdong Provience (2016KZDXM016), the Clinical Training Foundation of Southern Medical University (LC2016PY002), and the Innovative Foundation of Guangdong Province of China (2014KZDXM020).

References

Au-Yeung, B.B., Deindl, S., Hsu, L.Y., Palacios, E.H., Levin, S.E., Kuriyan, J., Weiss, A., 2009. The structure, regulation, and function of ZAP-70. Immunol. Rev. 228, 41–57.
Back, M., Hansson, G.K., 2015. Anti-inflammatory therapies for atherosclerosis. Nat. Rev. Cardiol. 12, 199–211.
Bhatt, A., Rohatgi, A., 2016. HDL cholesterol efflux capacity: cardiovascular risk factor and potential therapeutic target. Curr. Atheroscler. Rep. 18, 2.
Daugherty, A., Pure, E., Delfel-Butteiger, D., Chen, S., Leferovich, J., Roselaar, S.E., Rader, D.J., 1997. The effects of total lymphocyte deficiency on the extent of atherosclerosis in apolipoprotein E-/- mice. J. Clin. Invest. 100, 1575–1580.
Favari, E., Chroni, A., Tietge, U.J., Zanotti, I., Escola-Gil, J.C., Bernini, F., 2015. Cholesterol efflux and reverse cholesterol transport. Handb. Exp. Pharmacol. 224, 181–206.
Hashimoto-Tane, A., Saito, T., 2016. Dynamic regulation of TCR-microclusters and the microsynapse for T cell activation. Front. Immunol. 7, 255.
Hu, J., Luo, T., Xi, D., Guo, K., Hu, L., Zhao, J., Chen, S., Guo, Z., 2018. Silencing ZAP70 prevents HSP65-induced reverse cholesterol transport and NF-kappaB activation in T cells. Biomed. Pharmacother. 102, 271–277.
Hutchins, P.M., Heinecke, J.W., 2015. Cholesterol efflux capacity, macrophage reverse cholesterol transport and cardioprotective HDL. Curr. Opin. Lipidol. 26, 388–393.
Khera, A.V., Cuchel, M., de la Llera-Moya, M., Rodrigues, A., Burke, M.F., Jafri, K., French, B.C., Phillips, J.A., Mucksavage, M.L., Wilensky, R.L., et al., 2011. Cholesterol efflux capacity, high-density lipoprotein function, and atherosclerosis. N. Engl. J. Med. 364, 127–135.
Luo, T., Hu, J., Xi, D., Xiong, H., He, W., Liu, J., Li, M., Lu, H., Zhao, J., Lai, W., et al., 2016. Lck inhibits heat shock protein 65-Mediated reverse cholesterol transport in t cells. J. Immunol. (Baltimore, Md.: 1950) 197, 3861–3870.
McLaren, J.E., Michael, D.R., Ashlin, T.G., Ramji, D.P., 2011. Cytokines, macrophage lipid metabolism and foam cells: implications for cardiovascular disease therapy. Prog. Lipid Res. 50, 331–347.
Muslin, A.J., 2008. MAPK signalling in cardiovascular health and disease: molecular mechanisms and therapeutic targets. Clin. Sci. (Lond.) 115, 203–218.
Negishi, I., Motoyama, N., Nakayama, K., Nakayama, K., Senju, S., Hatakeyama, S., Zhang, Q., Chan, A.C., Loh, D.Y., 1995. Essential role for ZAP-70 in both positive and negative selection of thymocytes. Nature 376, 435–438.
Rahaman, S.O., Lennon, D.J., Febbraio, M., Podrez, E.A., Hazen, S.L., Silverstein, R.L., 2006. A CD36-dependent signaling cascade is necessary for macrophage foam cell formation. Cell Metab. 4, 211–221.
Ridker, P.M., Everett, B.M., Thuren, T., MacFadyen, J.G., Chang, W.H., Ballantyne, C., Fonseca, F., Nicolau, J., Koenig, W., Anker, S.D., et al., 2017. Antiinflammatory therapy with canakinumab for atherosclerotic disease. N. Engl. J. Med. 377, 1119–1131.
Rohatgi, A., Khera, A., Berry, J.D., Givens, E.G., Ayers, C.R., Wedin, K.E., Neeland, I.J., Yuhanna, I.S., Rader, D.R., de Lemos, J.A., et al., 2014. HDL cholesterol efflux capacity and incident cardiovascular events. N. Engl. J. Med. 371, 2383–2393.
Ross, R., 1999. Atherosclerosis–an inflammatory disease. N. Engl. J. Med. 340, 115–126.
Sabol, S.L., Brewer Jr, H.B., Santamarina-Fojo, S., 2005. The human ABCG1 gene: identification of LXR response elements that modulate expression in macrophages and liver. J. Lipid Res. 46, 2151–2167.
Seeger, F.H., Sedding, D., Langheinrich, A.C., Haendeler, J., Zeiher, A.M., Dimmeler, S., 2010. Inhibition of the p38 MAP kinase in vivo improves number and functional activity of vasculogenic cells and reduces atherosclerotic disease progression. Basic Res. Cardiol. 105, 389–397.
Tabas, I., Lichtman, A.H., 2017. Monocyte-macrophages and t cells in atherosclerosis. Immunity 47, 621–634.
Wang, H., Kadlecek, T.A., Au-Yeung, B.B., Goodfellow, H.E., Hsu, L.Y., Freedman, T.S., Weiss, A., 2010. ZAP-70: an essential kinase in T-cell signaling. Cold Spring Harb. Perspect. Biol. 2, a002279.
Wilhelm, A.J., Rhoads, J.P., Wade, N.S., Major, A.S., 2015. Dysregulated CD4+ T cells from SLE-susceptible mice are sufficient to accelerate atherosclerosis in LDLr-/- mice. Ann. Rheum. Dis. 74, 778–785.
Xue, X.H., Shi, F.F., Chen, T., Wei, W., Zhou, X.M., Chen, L.D., 2016. Inhibition of ERK1/2 improves lipid balance in rat macrophages via ABCA1/G1 and CD36. Mol. Med. Rep. 13, 1533–1540.
Yu, X.H., Fu, Y.C., Zhang, D.W., Yin, K., Tang, C.K., 2013. Foam cells in atherosclerosis. Clin. Chim. Acta 424, 245–252.
Zhang, L., Chen, Y., Yang, X., Yang, J., Cao, X., Li, X., Li, L., Miao, Q.R., Hajjar, D.P., Duan, Y., et al., 2016. MEK1/2 inhibitors activate macrophage ABCG1 expression and reverse cholesterol transport-an anti-atherogenic function of ERK1/2 inhibition. Biochim. Biophys. Acta 1861, 1180–1191.
Zhou, X., Nicoletti, A., Elhage, R., Hansson, G.K., 2000. Transfer of CD4(+) T cells aggravates atherosclerosis in immunodeficient apolipoprotein E knockout mice. Circulation 102, 2919–2922.